

Laboratory and Field Evaluations of the GeoAir2 Air Quality Monitor for Use in Indoor Environments

Dillon Streuber^a, Yoo Min Park^b, Sinan Sousan^{c,d,*}

^a*Environmental Health Sciences Program, Department of Health Education and Promotion, College of Health and Human Performance, East Carolina University, Greenville, NC 27858, USA*

^b*Department of Geography, Planning, and Environment, East Carolina University, Greenville, NC 27858, USA*

^c*Department of Public Health, Brody School of Medicine, East Carolina University, Greenville, NC 27834, USA*

^d*North Carolina Agromedicine Institute, Greenville, NC 27834, USA*

*Corresponding author. E-mail address: sousans18@ecu.edu (S. Sousan). Address: Carol-Belk Building, 300 Curry Ct, Greenville, NC 27858.

Abstract

Low-cost aerosol sensors open routes to exposure assessment and air monitoring in various indoor and outdoor environments. This study evaluated the accuracy of GeoAir2—a recently developed low-cost particulate matter (PM) monitor—using two types of aerosols (salt and dust), and the effect of changes in relative humidity on its measurements in laboratory settings. For the accuracy experiments, 32 units of GeoAir2 were used, and for the humidity experiments, 3 units of GeoAir2 were used, alongside the OPC-N3 low-cost sensor and MiniWRAS reference instrument. The normal distribution of slopes between the salt and dust aerosols was compared for the accuracy experiments. In addition, the performance of GeoAir2 in indoor environments was evaluated compared to the pDR-1500 reference instrument by collocating GeoAir2 and pDR-1500 at three different homes for five days. For salt and dust aerosols smaller than 2.5 μm ($\text{PM}_{2.5}$), both GeoAir2 ($r = 0.96\text{--}0.99$) and OPC-N3 ($r = 0.98\text{--}0.99$) were highly correlated with the MiniWRAS reference instrument. However, GeoAir2 was less influenced by changes in humidity than OPC-N3. While GeoAir2 reported an increase in mass concentrations ranging from 100% to 137% for low and high concentrations, an increase between 181% and 425% was observed for OPC-N3. The normal distribution of the slopes for the salt aerosols was narrower than dust aerosol, which shows closer slope similarities for salt aerosols. This study also found that GeoAir2 was highly correlated with the pDR-1500 reference instrument in indoor environments ($r = 0.80\text{--}0.99$). These results demonstrate potential for GeoAir2 for indoor air monitoring and exposure assessments.

38 **Keywords:** Particulate matter, PM2.5, Indoor air quality, SPS30 sensor, PM humidity effects.

39

ACCEPTED MANUSCRIPT

40 1 INTRODUCTION

41 The United States Environmental Protection Agency (EPA) identifies particulate matter
42 (PM) with a diameter of 2.5 μm or smaller in size ($\text{PM}_{2.5}$) as one of the criteria air pollutants.
43 $\text{PM}_{2.5}$ is of interest for its health effects and its ability to form from primary and secondary
44 emissions from reactions between other pollutants present in the air (EPA, 1990). Lifelong
45 exposure to PM can bring a host of negative health effects from silicosis related to silica exposure
46 and lung cancer linked to tobacco smoke (Collins et al., 2005; Slezakova et al., 2009). In
47 addition, elevated $\text{PM}_{2.5}$ concentrations are linked to mortality from heart disease, stroke, lung
48 cancer, chronic obstructive pulmonary disease and acute respiratory infections (Brook et al.,
49 2010; Hansel et al., 2016; Li et al., 2017; Huang et al., 2019; Kim et al., 2020). $\text{PM}_{2.5}$ is generated
50 from outdoor sources, such as mobile emissions, industrial activities, coal and biomass burning,
51 wildfires, dust and sea spray aerosols (Calvo et al., 2013), and indoor sources, such as cooking
52 practices, smoking, incense, candles, fireplace burning, and outdoor infiltration (Owen et al.,
53 1992; Marcé et al., 2018). It has been suggested that indoor air quality may be of greater health
54 risk than outdoor exposure (Cincinelli and Martellini, 2017), and indoor exposure to PM can
55 range over $500 \mu\text{g m}^{-3}$, causing serious health problems (Diapouli et al., 2008). Despite its
56 adverse health impacts, environmental, public health policies and research efforts have
57 historically focused on outdoor air quality due to its environmental effect, and relatively limited
58 attention has been paid to indoor air quality (WHO, 2010). However, in the U.S and other

59 industrialized countries, most people spend more than 80% of their time indoors (Franklin, 2007),
60 so developing methods/technologies to assess indoor exposure accurately and react accordingly is
61 critical.

62 Over the past few years, significant improvements in aerosol sensor technologies have
63 allowed researchers to capture exposure in indoor environments for better accuracy. The air
64 sensor technologies come in various forms, including real-time optical particle counters (OPCs),
65 photometers, and spectrometers (Sousan et al., 2016b). OPCs use light scattering technology to
66 detect particles of different sizes and calculate mass concentration compared to photometers that
67 determine the mass concentration based on the reflected light from a bulk of particles. However,
68 their high prices (\$3,000–\$100,000) have relegated these devices to research and industrial
69 application. These limitations create a large monetary barrier for communities and individuals
70 interested in providing representation for themselves and those around them. As a result, many
71 individuals go unrepresented as to their exposure (Jiao et al., 2015). There has been a trend in
72 developing low-cost aerosol sensors to open the description of exposures to individuals to
73 represent their indoor air quality (Popoola et al., 2018).

74 Low-cost OPCs can provide accessibility to air quality representation to individuals that
75 cannot afford the higher cost sensors. An added benefit is the tendency to be lightweight and
76 smaller in size, providing the opportunity to deploy these sensors indoors for personal use

77 compared to their higher-cost counterparts (Sousan et al., 2021). These low-cost sensors include
78 the OPC-N3 (Alphasense, Essex, Great Notley, United Kingdom) and the SPS30 (Sensiron AG,
79 Stäfa, Switzerland). Tryner et al. (2020) tested the SPS30 and showed consistent readings for dust
80 $PM_{2.5}$ concentrations over the long periods and higher precision than other low-cost OPCs.
81 Sousan et al. (2021) reported a high correlation ($r = 0.99$) for the SPS30 and OPC-N3 compared
82 to the reference instrument in environmental and occupational settings with a moderate bias for
83 salt aerosol $PM_{2.5}$ measurements after testing three pairs of SPS30 and OPC-N3. Other low-cost
84 OPCs include the Plantower PMS5003, Dylos, Honeywell HPMA115S0 and PM Nova that have
85 been evaluated in laboratory and field settings (Sousan et al., 2016b; Levy Zamora et al., 2019;
86 Hong et al., 2021; Dubey et al., 2022)

87 Although low-cost OPCs are promising, environmental conditions can affect their
88 classification of particles (Crilley et al., 2018; Crilley et al., 2020). For example, in high relative
89 humidity conditions, hygroscopic growth can sheathe a particle in a layer of water (Svenningsson
90 et al., 1992). However, the true size does not matter in inhalation. This overestimated size is the
91 actual size that people inhale in humid conditions. Therefore, OPCs can misclassify a particle as
92 larger than its true size, causing it to overestimate the mass of detected aerosol (Crilley et al.,
93 2018). Although previous studies have performed experiments on various low-cost sensors
94 alongside the SPS30 to determine the effect of changing relative humidity on reported $PM_{2.5}$

95 concentration against reference instruments such as a TEOM (Wang et al., 2021), they have not
96 derived correction equations for the SPS30 from this change in relative humidity with mass
97 concentration. To support assessments of disease burden from indoor aerosols, reliable and
98 accurate indoor air quality monitoring should be preceded.

99 The objectives of this study are 1) to determine the accuracy of 32 SPS30's built in the GeoAir2–
100 –a low-cost, GPS-enabled, portable air-monitoring platform (Park et al., 2021)—using salt and dust
101 aerosols in laboratory settings; 2) to identify the effect of relative humidity on GeoAir2's PM_{2.5}
102 mass concentrations using salt aerosol in laboratory settings; and 3) to evaluate the GeoAir2's real-
103 time indoor PM_{2.5} readings in three individuals' homes compared to those of a filter-corrected real-
104 time reference instrument to determine the accuracy in indoor environments. This study provides
105 the required assessment for the GeoAir2 and necessary data that position the instrument as a viable
106 air quality monitor for indoor settings and possible outdoor use.

107

108 **2 MATERIALS AND METHODS**

109 The specifications and differences for the low-cost and reference instruments are shown in Table

110 1.

Technical Data	GeoAir2	OPC-N3	pDR-1500	MiniWRAS
Cost (\$)	300	500	7,000	30,000

Size range (μm)	0.30–10.00	0.30–40.00	One size based on cyclone	0.01–35.00 \
Type (active or passive flow)	Active	Active	Active	Active
Bin size (software bins, dimensionless)	5	24	-	41
Concentration range ($\mu\text{g m}^{-3}$)	0–1,000	0–2,000	0.001–400,000	0–100,000
Mass concentration measurement	PM ₁ , PM _{2.5} , PM ₁₀	PM ₁ , PM _{2.5} , PM ₁₀	PM ₁ , PM _{2.5} , PM ₁₀	PM ₁ , PM _{2.5} , PM ₁₀
Sampling flow rate (Liters per minute)	-	-	1.52	1.20
Number concentration	Yes	Yes	No	Yes
Sampling frequency	1 s	1 s	1 s	1 min
Internal rechargeable battery	Yes	No	Yes	Yes
Dimensions: L × W × H (m)	0.055 × 0.140 × 0.0375	0.075 × 0.006 × 0.060	0.181 × 0.143 × 0.0484	0.34 x 0.31 x 0.12

111

112

113

114 **2.1 Low-Cost Sensors**

115 **2.1.1 GeoAir2**

116 The GeoAir2 (East Carolina University, Greenville, NC, USA) is a recently developed portable
117 air-monitoring platform that provides geo-referenced real-time PM_{2.5} concentrations by combining
118 air sensors and a GPS module. The monitor costs \$250-\$350 depending on the units ordered (Park
119 et al., 2021). It uses the SPS30 for PM_{2.5} monitoring, includes volatile organic compound (VOC)
120 and hydrogen H₂-based carbon dioxide (CO₂) sensors, and provides temperature, humidity, time,
121 and GPS logging. The SPS30 has five bins from 0.3 μm to 10 μm, converted to number counts and
122 mass concentrations using proprietary equations (Sensirion, 2020). Compared to other
123 commercially available devices existing in the market, the benefit of using GeoAir2 for this study
124 is that it can be used at any indoor places with limited or no Wi-Fi access because it does not require
125 Wi-Fi access and have to rely on smartphone applications to transfer data. In addition, encrypted
126 data files are stored on a microSD card inside the platform.

127 **2.1.2 OPC-N3**

128 The OPC-N3 costs \$500 and features 24 bins from 0.35 μm to 40 μm which are converted into
129 number counts and mass concentrations with algorithms developed by the company to measure
130 mass concentrations of particles from 0 to 2000 μg m⁻³ (Alphasense, 2019). The device also features
131 built-in temperature and relative humidity sensors and an internal fan. However, it does not feature
132 an internal battery, so power must be supplied. The OPC-N3 specifications are included in Table
133 1, and its small form-factor allows for easy deployment. However, the device requires an external

134 power source and a dedicated computer to retrieve time-stamped data, where the OPC-N3 does not
135 have an internal clock (Alphasense, 2019).

136

137 **2.2 Reference Instruments**

138 **2.2.1 pDR-1500**

139 The personal DataRAM (pDR-1500, Thermo Fisher Scientific, Waltham, Massachusetts, USA) is
140 a photometer that uses a cyclone to measure particulate mass concentration at a specific particle
141 size (Thermo., 2016). The device is a reference instrument, providing a filter to correct real-time
142 data. The pDR is equipped with a 37 mm fiberglass filter (Whatman, CATNon.1827-037,
143 Maidstone, United Kingdom) for particle collection that can then be removed and weighed for
144 gravimetric analysis.

145 **2.2.2 MiniWRAS**

146 The GRIMM Mini Wide Range Aerosol Spectrometer (MiniWRAS, GRIMM Aerosol Technik
147 Ainring GmbH & Co. KG, Ainring, Germany) uses a corona charge to measure particles smaller
148 than 0.25 μm by supplying unipolar ions to charge the aerosol and measure the charge using a
149 Faraday Cup Electrometer. Particles between 0.25 and 35 μm are measured using an optical
150 sensor (GRIMM, 2021). The device reports number concentrations in 41 bins, including PM_{2.5}
151 mass concentrations.

152

153 **2.3 Experimental Setup to Evaluate the Accuracy, Bias and Precision**

154 **2.3.1 Chamber Description**

155 The experiments were performed inside a controlled, airtight, plexiglass exposure chamber with
156 dimensions $1.82\text{ m} \times 0.66\text{ m} \times 0.66\text{ m}$ ($L \times W \times H$) as shown in Figure 1. This chamber was split
157 into a mixing/dilution zone and a sampling zone. Both zones were split by a honeycomb
158 straightening section (AS100, Rusken, Grandview, MO, USA). The mixing/dilution zone
159 measured $0.61\text{ m} \times 0.61\text{ m} \times 0.66\text{ m}$ ($L \times W \times H$) with an inlet on both the bottom and side to
160 introduce generated aerosol. Mixing was accomplished with two small fans in this zone. Particle-
161 free air was supplied for the mixing process by two High Efficiency Particulate Air (HEPA)
162 filters (99.99% efficiency rating each). The sampling zone measured $0.61\text{ m} \times 0.61\text{ m} \times 0.66\text{ m}$
163 ($L \times W \times H$), leading to a vacuum outlet that exhausted air through two HEPA filters. A valve on
164 the exhaust outlet allowed adjustment of the flow rate through the sampling zone. During the
165 experiment, 32 GeoAir2, 6 OPC-N3's, and the pDR-1500 (equipped with a $2.5\text{ }\mu\text{m}$ cyclone - 50%
166 cut-point) were located directly within the sampling zone of the chamber. The MiniWRAS was
167 placed outside the chamber with a sampling probe inside the sampling zone.

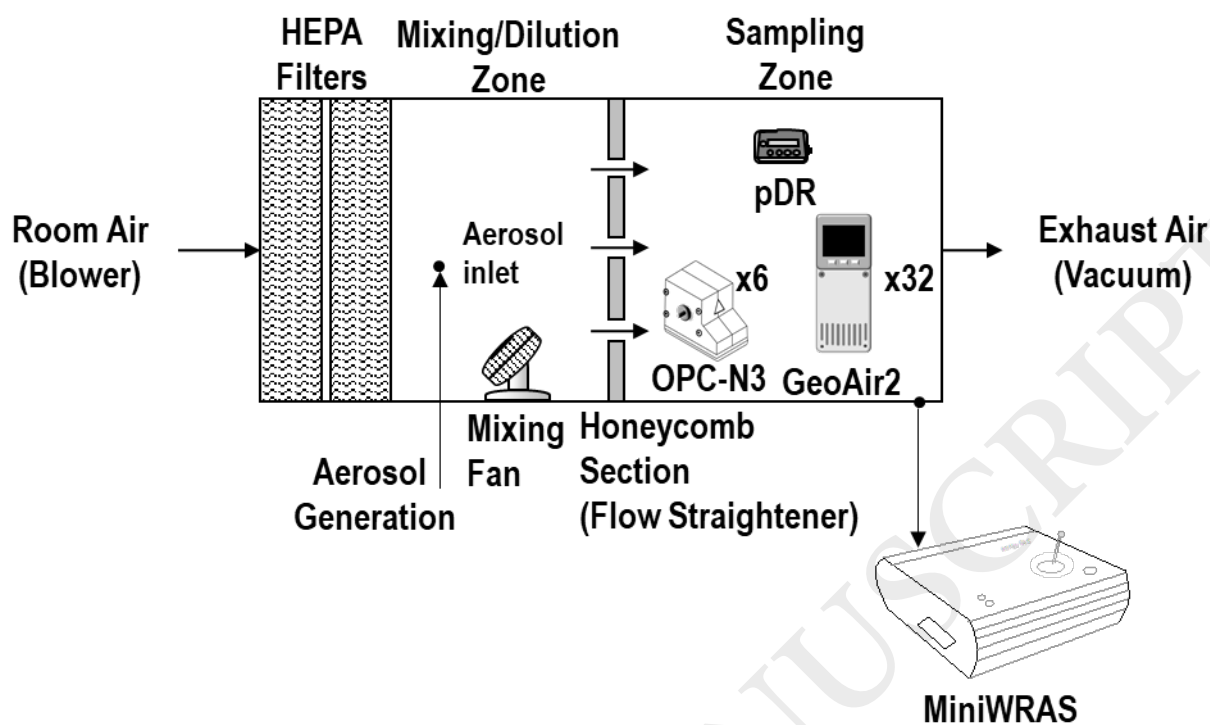


Figure 1. The experimental chamber used to test the sensors for salt and dust particulate matter detection.

168

169 2.3.2 Aerosol Generation

170 Salt and dust aerosols were generated using different generation methods. Salt was chosen for its

171 wide use and relative safety to help evaluate the GeoAir2 units (Sousan et al., 2016b). Salt

172 aerosol was generated with the Aerogen nebulizer (Aerogen, Galway, Connacht, Ireland) using a

173 2% (by wt.) solution of NaCl. A mass flow controller (Cole-Parmer 32907-73, Antylia Scientific,

174 Vernon Hills, Illinois, USA) supplied particle-free air from a five-stage desiccant into a silica

175 column. Then, the salt aerosol was passed through a silica column to remove moisture, and dry

176 salt particles entered the mixing zone of the chamber, where particle-free air was introduced to
177 achieve the desired steady-state concentrations.

178 The second aerosol chosen was Arizona Road Dust (ARD; PTI ID: 13328B, Powder
179 Technology Inc, MN, USA) due to its wide use and similarity to coarse mineral dust found in
180 indoor settings. The aerosol was generated utilizing the Vilnius Aerosol Generator (VAG, CH
181 Technologies, Westwood, New Jersey, USA). The VAG dispenses dry powder to produce aerosol
182 concentrations from 1 to 2500 mgm⁻³. ARD was loaded into the device 1.33 g at a time, and once
183 assembled, particle-free air was supplied and controlled by the same mass flow controller
184 mentioned above. This mixture was supplied directly into the mixing zone of the chamber with
185 particle-free air to achieve the desired steady-state concentrations.

186 The GeoAir2, OPC-N3, and pDR-1500 were set to record real-time measurements with
187 one-second frequency, while the MiniWRAS recorded every one minute. The pDR-1500 also
188 provided 37 mm filters pre- and post-weighed before and after the experiments using a Mettler
189 Toledo microbalance (Model: XPR26DR, Columbus, Ohio, USA) and anti-static kit with a large
190 U-electrode (Model: 63052302, Mettler Toledo, Columbus, Ohio, USA). The pDR-1500 operated
191 at a flow rate of 1.52 LPM across all experiments.

192 All sensors were operated in particle-free air to achieve a concentration of 0 µg m⁻³ for
193 five minutes before steady-state concentrations were achieved at 10, 20, 30, 40, 50, 100, 200,

194 300, 400, and 500 $\mu\text{g m}^{-3}$. The laboratory experiments were performed to simulate indoor
195 conditions at low (up to 50 $\mu\text{g m}^{-3}$) and high (up to 500 $\mu\text{g m}^{-3}$) concentrations. Calibrating
196 sensors at low and high concentrations have shown calibration differences, which justifies
197 performing these separately (Sousan et al., 2021). Since the World Health Organization
198 guidelines for air quality recommend a 25 $\mu\text{g m}^{-3}$ 24-hour mean for $\text{PM}_{2.5}$, twice the value of 50
199 $\mu\text{g m}^{-3}$ was chosen as the upper limit for low concentration (WHO, 2010). The high concentration
200 was based on the literature previously mentioned in the Introduction (Diapouli et al., 2008). The
201 pDR-1500 was used to monitor the steady-state concentrations achieved with salt and ARD
202 aerosol. Aerosol size distribution of the SPS30 inside the GeoAir2, OPC-N3, and MiniWRAS
203 were measured for salt and ARD aerosols in a previous study conducted by the author's (Sousan
204 et al., 2021), therefore, these measurements were not included in this work.

205

206 **2.4 Experimental Setup to Determine the Effect of Relative Humidity**

207 **2.4.1 Chamber Description**

208 The chamber used for the accuracy and bias assessment was too large to perform and control a
209 humidity experiment. Therefore, smaller chambers were used for the humidity test. The relative
210 humidity experiments were performed within two controlled, airtight Polyvinyl Chloride
211 chambers measuring 0.36 m \times 0.30 m \times 0.22 m (L \times W \times H) and connected by a 9.5 mm hose.
212 Positive pressure was used to move air from the mixing chamber into the sampling chamber, as

213 shown in Figure 2. The mixing chamber featured two inlets: a first inlet for humidified air
214 regulated by a Miller-Nelson control system (Miller Nelson Analytical HCS-501, Brentwood,
215 California, USA) and a second inlet connected to an aerosol generator. The sampling chamber
216 featured a single inlet and a single outlet that led to a HEPA filter. The GeoAir2 and OPC-N3
217 were placed inside the sampling chamber, while the MiniWRAS sampling probe was connected
218 to a silica drying column which was then attached to an outlet in the sampling chamber. The
219 objective was to compare the low-cost sensor measurements with dry particle concentrations
220 measured by the MiniWRAS since all instruments are optical sensors and are affected by
221 humidity changes. Three pairs of GeoAir2 and OPC-N3 were used in the humidity tests
222 considering space constraints within the chamber, exposing each to the generated aerosol.
223

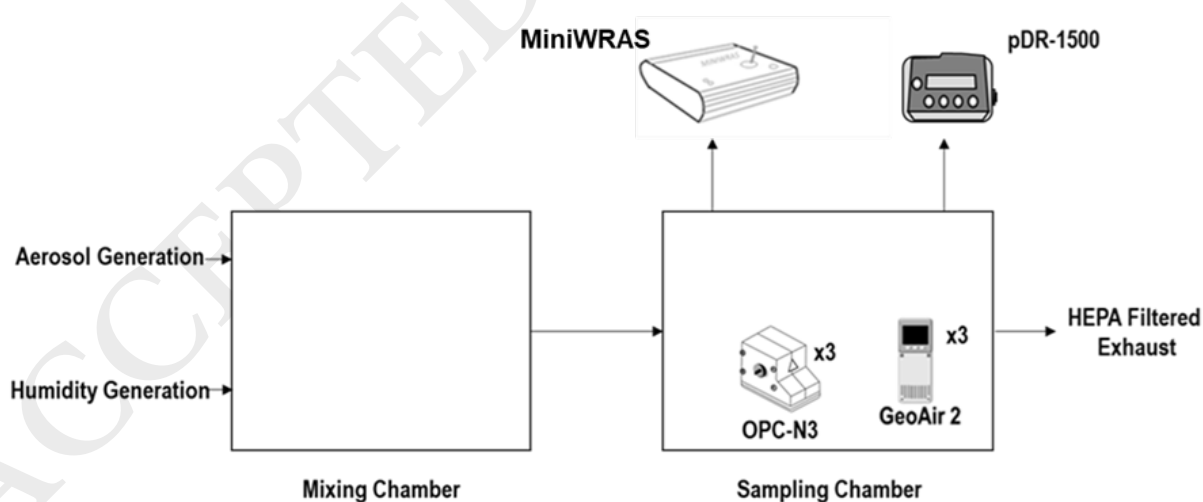


Figure 2. Experimental chamber designed to test the effects of different relative humidity levels on sensor reading of particulate mass.

224

225 **2.4.2 Aerosol Generation and Humidity Change**

226 Salt aerosol was generated using a Collison nebulizer (CH Technologies, Westwood, NJ, USA).

227 The nebulizer was operated using the same mass flow controller mentioned above with a 2% (by

228 wt.) solution of NaCl. Sensors were operated in particle-free air to achieve a $0 \mu\text{g m}^{-3}$ steady-state

229 concentration for five minutes. Steady-state concentrations of salt aerosol were achieved at 25,

230 50, 75, and $100 \mu\text{g m}^{-3}$ across five relative humidity levels of 30, 50, 70, 80, and 90% with the

231 Miller-Nelson. These steady-state concentrations were held for five minutes and monitored in

232 real-time with the MiniWRAS.

233

234 **2.5 Field Deployment in Indoor Residential Environments**

235 Indoor exposure constitutes a different range of aerosol sources: cigarettes and electronic

236 cigarettes, cooking oil, burning wood, incense, and possible outdoor sources such as dust and

237 wood smoke (Kulkarni et al., 2011). Therefore, the study team recruited 3 participants to deploy

238 air monitors in their homes in partnership with the Association of Mexicans in North Carolina

239 (Greenville, NC). Indoor air quality was monitored for 5 days at three different homes. We

240 recruited individuals who spend the majority of their time inside their homes because 1) daily

241 activities they undertake at home (e.g., cooking) would allow the study team to obtain both low

242 and high concentration data and 2) the study team had to visit their home every day during the

243 study to change the filter in the pDR-1500 every 24 hours. A single GeoAir2 unit was placed
244 alongside a field blank filter and a pDR-1500 equipped with a cyclone for measuring PM_{2.5} and a
245 37-mm fiberglass filter (Whatman, CATNon.1827-037, Maidstone, United Kingdom) for
246 gravimetric analysis. The sampling location within the home was chosen based on the vicinity to
247 regularly occupied living space and household activities such as cooking, where the kitchen was
248 open to the living room. These locations were set upon tables in the living room, giving the
249 devices a height comparable to a seated person. The living room next to an open kitchen for each
250 house was chosen to quantify the exposure for those seated in the living area from activities in the
251 kitchen. Photographs were not taken inside the homes to protect the privacy of the residents.

252

253 **2.6 Data Analysis**

254 **2.6.1 Accuracy, Bias and Precision**

255 PM_{2.5} data for 32 GeoAir2 devices were averaged over one-minute and time-paired to create
256 representative tables and figures for each dataset and compared directly to the MiniWRAS
257 reference device alongside the OPC-N3 and pDR-1500. The average measurement from the 32
258 GeoAir2 and 6 OPC-N3's were analyzed to determine slope, intercept, correlation coefficient (r),
259 coefficient of determination (r²), Bias and coefficient of variation (CV). The average
260 measurements were compared to the MiniWRAS reference device for both data sets, salt and
261 ARD aerosols. The statistics were calculated for both low and high concentration data. The

262 MiniWRAS data were filter-corrected by calculating the correction factor, the filter mass
263 concentration divided by the average MiniWRAS real-time measurements. After this analysis, a
264 comparison was made to EPA and National Institute for Occupational Safety and Health
265 (NIOSH) acceptance criteria which include a slope of 1.0 ± 0.1 , an intercept of $0 \pm 5 \mu\text{g m}^{-3}$
266 (EPA), $r \geq 0.97$, a bias percentage of $\pm 10\%$ (NIOSH), and CV values up to 10% (EPA) (NIOSH,
267 2012; EPA, 2016; Sousan et al., 2016b; Sousan et al., 2021). Bias and CV values were calculated
268 using the following equations:

$$269 \quad \% \text{ Sensor Bias} = (\text{Sensor} - \text{MiniWRAS}) / \text{MiniWRAS} \times 100 \quad (1)$$

$$270 \quad \text{CV} = \text{Standard Deviation} / \text{Sensor} \quad (2)$$

271 where Sensor is the average value reported by the low-cost sensors for the given minute of
272 steady-state. MiniWRAS is the filter-corrected value reported by the MiniWRAS for the given
273 minute of steady-state. Standard Deviation is the standard deviation between the individual
274 sensors.

275 **2.6.2 Slope Analysis**

276 For each experiment, for low and high concentrations of salt and ARD aerosol, 50% of the
277 sensors were chosen that fall within the mean slope value to identify possible sensors that can be
278 calibrated using one correction factor (slope value) for all experiments. Finally, we identified the
279 sensors that can be chosen for field deployment using one calibration slope factor if the slope
280 values fall within less than a Z% of the mean slope for at least three experiments. The Z value is

281 determined by slopes derived from the GeoAir2. Finally, a normal distribution curve was created
282 to collectively compare the range of slope values reported from the salt and ARD experiments for
283 low and high concentrations.

284 **2.6.3 Humidity Correction**

285 The reported concentrations of PM_{2.5} by the low-cost sensors were averaged between the
286 achieved steady states to provide a mean value that could then be compared to the MiniWRAS
287 reference device. SPSS was used to analyze variance and a Tukey post hoc test to derive
288 regression equations between humidity and mass concentrations.

289 **2.6.4 Field Evaluation**

290 After deployment, pDR-1500 real-time data was filter-corrected, similar to the MiniWRAS. In
291 addition, a time-series plot was created for the GeoAir2 data with the filter-corrected pDR-1500
292 data for the three-home deployments. The slope, intercept, and r^2 values were calculated for each
293 home.

294

295 **3 RESULTS AND DISCUSSION**

296 **3.1 Accuracy, Bias and Precision**

297 Accuracy results between the three instruments compared to the MiniWRAS reference
298 device are shown in Table 2 for salt and ARD aerosols. During salt generation, the GeoAir2,
299 OPC-N3, and pDR-1500 maintained a high correlation with the MiniWRAS reference device,
300 suggesting a linear regression, although slope variation remained high between devices. Both
301 low-cost sensors met acceptance criteria based on intercept and r value for low concentrations of

302 salt and ARD aerosols. However, the only device that fully met EPA acceptance criteria of the
 303 slope, intercept, and r value was the GeoAir2 during low ARD aerosol concentrations, though it
 304 did not meet NIOSH bias criteria. Bias calculations suggest that the GeoAir2 consistently
 305 underestimated both aerosols and concentrations, while the OPC-N3 overestimated salt aerosol.
 306 These findings remained consistent with previous findings in Sousan et al. (2021), with
 307 correlation values remaining greater than 0.96. Nguyen et al. (2021) also produced a similar
 308 result, an r^2 of 0.95 for the SPS30 PM_{2.5} measurements.
 309

Table 2. Evaluation of average correlation factors across measuring devices compared to the MiniWRAS reference device during tests involving salt and ARD aerosols at low and high concentrations^a. Relative humidity ($35 \pm 5\%$) and temperature ($23 \pm 2^\circ\text{C}$) were at normal room conditions.

Concentration	Instrument	No. of Samples	Slope	Intercept	r	r ²	%Bias	%CV
Salt Low								
Concentration	pDR	36	1.12	0.42	0.99	0.98	14.47	
	OPC-N3	36	0.67	0.82	0.98	0.86	-28.10	39.82
	GeoAir2	36	0.53	-0.46	0.96	0.93	-49.34	20.58
Salt High								
Concentration	pDR	36	0.66	11.10	0.97	0.94	-25.17	

OPC-N3	36	0.72	-24.33	0.99	0.99	-37.78	49.50
GeoAir2	36	0.34	20.23	0.98	0.97	-51.52	20.16

ARD Low

Concentration	pDR	36	1.67	-2.58	0.99	0.99	51.53
	OPC-N3	36	2.33	0.13	0.99	0.99	134.83
	GeoAir2	36	0.99	-2.86	0.99	0.99	-18.67

ARD High

Concentration	pDR	36	1.48	18.17	0.98	0.97	64.11
	OPC-N3	36	1.91	27.93	0.99	0.98	112.40
	GeoAir2	36	0.85	6.71	0.99	0.98	-9.24

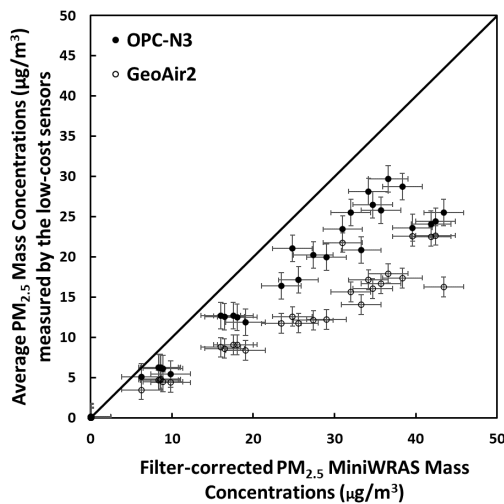
^aThe low concentrations are considered to be 0 to 50 $\mu\text{g m}^{-3}$ based on EPA's PM_{2.5} standard for 35 $\mu\text{g m}^{-3}$, while high concentrations are considered to be 50 to 500 $\mu\text{g m}^{-3}$ in this experiment.

310

311 The scatter plots for the average low-cost PM_{2.5} measurements compared to the filter-
312 corrected MiniWRAS PM_{2.5} measurements for low and high salt concentrations are shown in
313 Figure 3. Salt aerosol exposure showed a distinct tendency to underestimate in both low-cost
314 sensors compared to the MiniWRAS reference device. However, the OPC-N3 showed to
315 underestimate less severely than the GeoAir2. This trend was visible in low and high
316 concentrations of salt aerosol, with sensors tending to underestimate. These results were

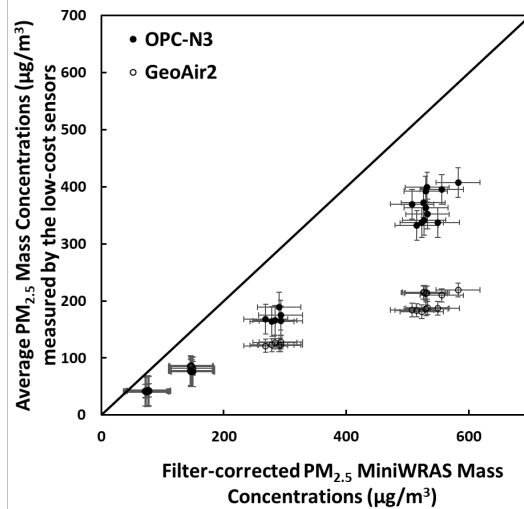
317 consistent with previous findings in Sousan et al. (2021), where readings from the OPC-N3
318 during PM_{2.5} salt aerosol experiments were underestimated compared to the MiniWRAS
319 reference device but less so than for the GeoAir2. Sousan et al. (2021) observed that the SPS30
320 slightly overestimated PM_{2.5} concentrations compared to non-filtered MiniWRAS concentrations,
321 and underestimated PM_{2.5} concentrations compared to filtered MiniWRAS concentrations.
322 Therefore, this indicates that the raw GeoAir2 is comparable to the raw MiniWRAS data, and
323 these results are affected by the salt filter correction factor. The OPC-N3 has been known to
324 underestimate during experiments with other aerosols, including welding fumes which are fine
325 particles (Sousan et al., 2016a).
326

a) Salt at low concentrations



c) ARD at low concentrations

b) Salt at high concentrations



d) ARD at high concentrations

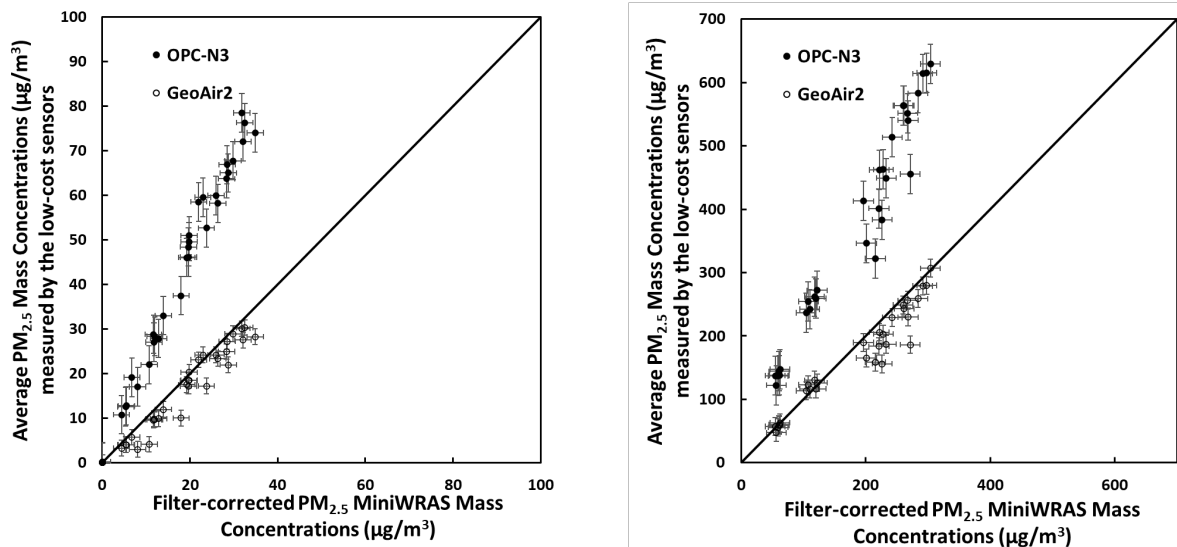


Figure 3. The average PM_{2.5} mass concentrations measurements by the low-cost sensors compared to the filter-corrected MiniWRAS measurements for a) salt at low concentrations, b) salt at high concentrations, c) ARD at low concentrations and d) ARD at high concentrations. Relative humidity ($35 \pm 5\%$) and temperature ($23 \pm 2^\circ\text{C}$) were at normal room conditions.

327 The scatter plots for low and high ARD concentrations showed a tendency of
 328 overestimation by the OPC-N3 compared to the MiniWRAS reference device (Figure 3), which is
 329 consistent with previous findings in Sousan et al. (2021). The GeoAir2 monitor was significantly
 330 closer to the MiniWRAS reference device during ARD generation than the salt generation,
 331 though it was slightly underestimated. These results yielded a linear relationship between the
 332 GeoAir2 and the MiniWRAS. This result is slightly different from the one in Sousan et al.
 333 (2021), which concluded that SPS30 significantly underestimated concentrations of ARD
 334 compared to the MiniWRAS. However, the results of the current study are more reliable because

335 we tested 32 units of SPS30, while 3 units were tested in the previous study. The findings of this
336 study suggest that the GeoAir2 is a more suitable platform for measuring indoor dust aerosol than
337 the OPC-N3.

338

339 **3.2 Slope Analysis**

340 Comparing the reported slope values of each GeoAir2 device to the mean slope of each
341 respective experiment showed that only 19 devices met the criteria three or more times.
342 Therefore, an interval of $Z = 20\%$ was chosen to allow at least half of the devices to report at
343 least two mean slopes within the acceptable threshold. The mean slopes for low and high
344 concentrations of salt and ARD were 0.53, 0.33, 0.98, and 0.8, respectively. Similar results have
345 been produced in a larger-scale calibration using Sharp low-cost sensors (GP2Y1010AU0F,
346 Sharp Electronics, Osaka, Japan) (Sousan et al., 2018).

347 The salt and ARD normal distributions for all the slopes, low and high concentrations, of
348 the GeoAir2 are displayed in Figure 4. These results show that when the GeoAir2 was calibrated
349 with salt, all the sensors underestimated the true concentrations for low and high concentrations.
350 In contrast, when the GeoAir2 was calibrated with ARD, 53% of the sensors underestimated the
351 low concentrations and 75% underestimated the high concentrations. Therefore, the range of
352 slopes reported for salt aerosol was narrower than for ARD aerosol. It may be because the
353 manufacturer calibrates the SPS30 with salt aerosol (Sousan et al., 2021). In addition, the results

354 show that calibration by one aerosol cannot be considered universal for other aerosols. These
355 results are similar to other studies that have shown that calibration equations are dependent on
356 aerosol type (Wang et al., 2015; Sousan et al., 2016a; Sousan et al., 2016b). Therefore,
357 calibration would be best performed on-site with the aerosols expected. This unexpected variation
358 in slope may affect the deployment of sensors based on calibration by non-target aerosol for
359 indoor use.
360

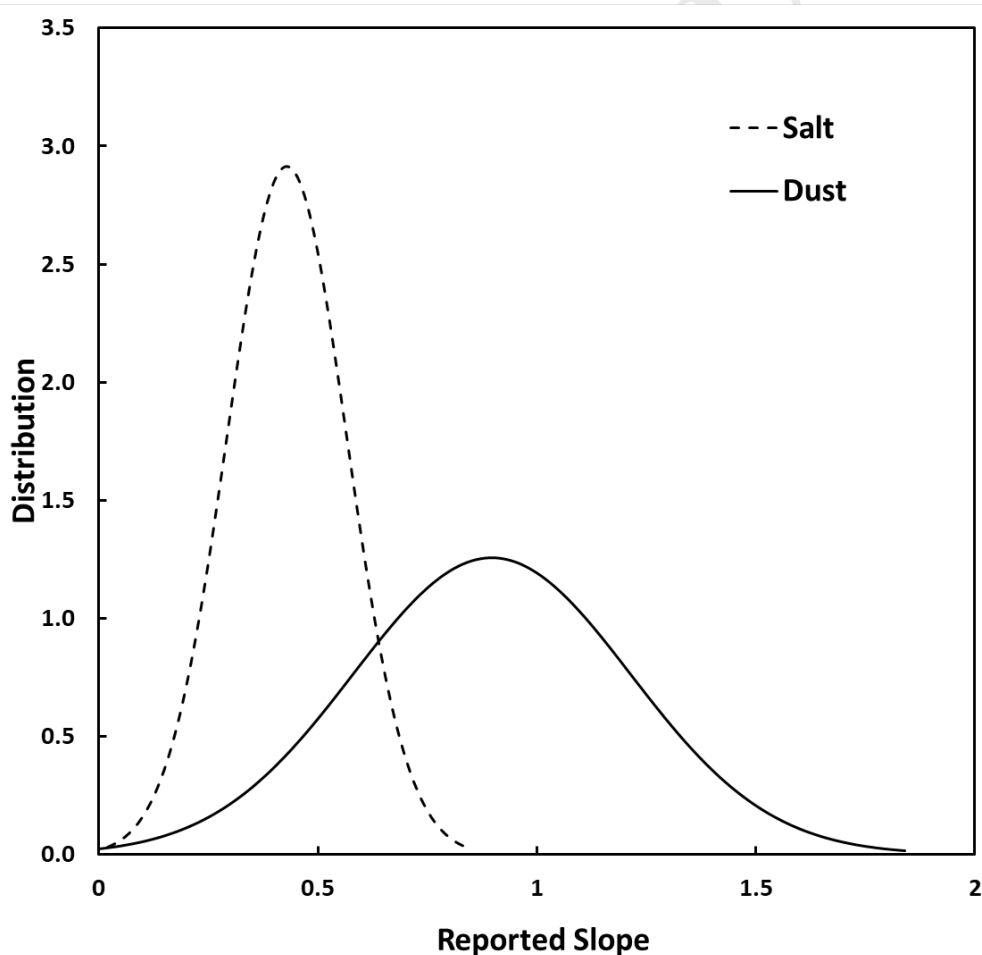


Figure 4. The normal distribution of slopes was recorded by the GeoAir2 units across all salt aerosol testing.

361

362 **3.3 Humidity Correction**

363 $PM_{2.5}$ mass concentrations of the OPC-N3 and GeoAir2 compared to the MiniWRAS at
364 different humidity levels are shown in Figure 5. For the OPC-N3, humidity effects were large,
365 where $PM_{2.5}$ mass concentrations increased 425% for low concentrations (25 to $50 \mu\text{g m}^{-3}$) and
366 181% for high concentrations (75 to $100 \mu\text{g m}^{-3}$) when the humidity changed from 50% to 90%,
367 respectively. For the GeoAir2, the humidity effects were much lower, where $PM_{2.5}$ mass
368 concentrations increased 100% for low concentrations and 137% for high concentrations when
369 the humidity changed from 50% to 90%, respectively. The change in relative humidity increased
370 the overestimation for both low-cost sensors due to hygroscopic growth in both low and high
371 concentrations. The increase in magnitude was also found in another study (Zou et al., 2021).
372 This level of hygroscopic growth was also observed for the SPS30 and OPC-N3 in Wang et al.
373 (2021).

a) OPC-N3

b) GeoAir2

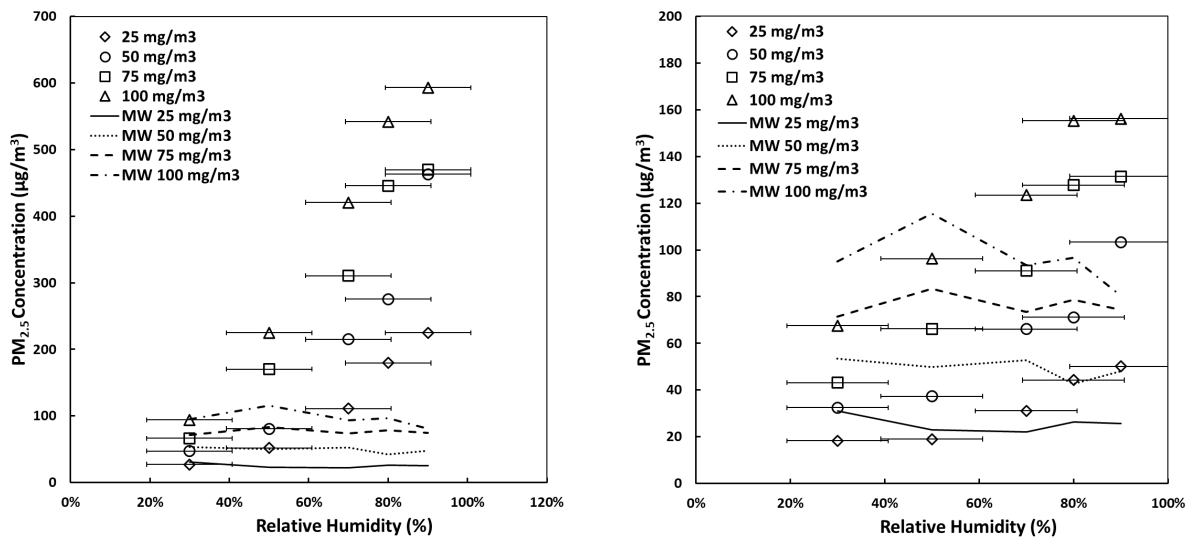


Figure 5: Relative humidity (%) effects on $PM_{2.5}$ concentrations ($\mu g m^{-3}$) detected by the a) OPC-N3 and b) GeoAir2 compared to the MiniWRAS (MW) $PM_{2.5}$ concentration at different steady states of salt aerosol. The MW was not affected by the humidity because the particles were dried before measurements were performed.

374

375 Humidity correction equations were developed for the OPC-N3 and GeoAir2:

376 OPC-N3 Measured $PM_{2.5}$ ($\mu g m^{-3}$) = $-371.13 + 3.38\text{Concentration} + 6.42\text{Humidity}$ (3)

377 ($R^2 = 0.91$)

378 GeoAir2 Measured $PM_{2.5}$ ($\mu g m^{-3}$) = $-73.26 + 1.17\text{Concentration} + 1.20\text{Humidity}$ (4)

379 ($R^2 = 0.93$)

380 where the Concentration is a steady-state concentration achieved (range 25–100 $\mu g m^{-3}$) and

381 Humidity is relative humidity achieved (range 30 to 90%). These results show that the GeoAir2

382 device is less affected by the change in relative humidity than the OPC-N3. The data suggest that

383 compared to the OPC-N3, the GeoAir2 is not only a better option for indoor settings, but also a
384 better option for use in environmental conditions where the relative humidity is expected to be
385 high or variable such as outdoor settings.

386

387 **3.4 Field Evaluation**

388 The time series plot of the pDR-1500 and GeoAir2 measurements in indoor settings is
389 shown in Figure 6. The Home 2 plot represents 4-day data because the GeoAir2 failed to log for
390 one day. There was also a loss of data for Home 3 because the pDR-1500 lost power for one day.
391 The pDR-1500 data were corrected with the filter measurements when the filters were above the
392 limit of detection of 0.50 mg. The r^2 values were lower in Homes 2 and 3, which may be related
393 to the loss of data and the smaller sample size. Therefore, it is expected that the presence of this
394 data would have increased the r^2 values to levels comparable to the r^2 value of 0.99 for Home 1.
395 The increase of side-by-side sampling time has been shown to increase correlation, as suggested
396 by Sousan et al. (2018). These results provide a higher correlation than those found by Demanega
397 et al. (2021), with slopes of indoor PM_{2.5} concentrations compared to the estimated true
398 concentration ranging from 0.22 to 0.82. The full set of data collected at Home 1 indicates that
399 the high correlation between readings from the GeoAir2 and the filter-corrected pDR-1500
400 suggests that the GeoAir2 is a promising low-cost sensor for residential use. Future work will test
401 GeoAir 2 in non-residential, indoor settings.

402 Optical sensors are affected by aerosol type where the sensor performance differs based
403 on aerosol refractive index, particle size and shape. Previous studies have discussed the
404 difference between aerosol types and optical sensor performance (Sousan et al., 2016a; Sousan et
405 al., 2016b). These studies emphasized that the performance of optical sensors is considerably
406 superior for non-light-absorbing particles such as salt and dust when compared to light-absorbing
407 particles such as diesel and welding fumes. Therefore, the GeoAir2 sensor would be suitable for
408 measuring aerosols produced from cigarettes, cooking oil, incense, and dust, compared to soot
409 particles from burning wood.

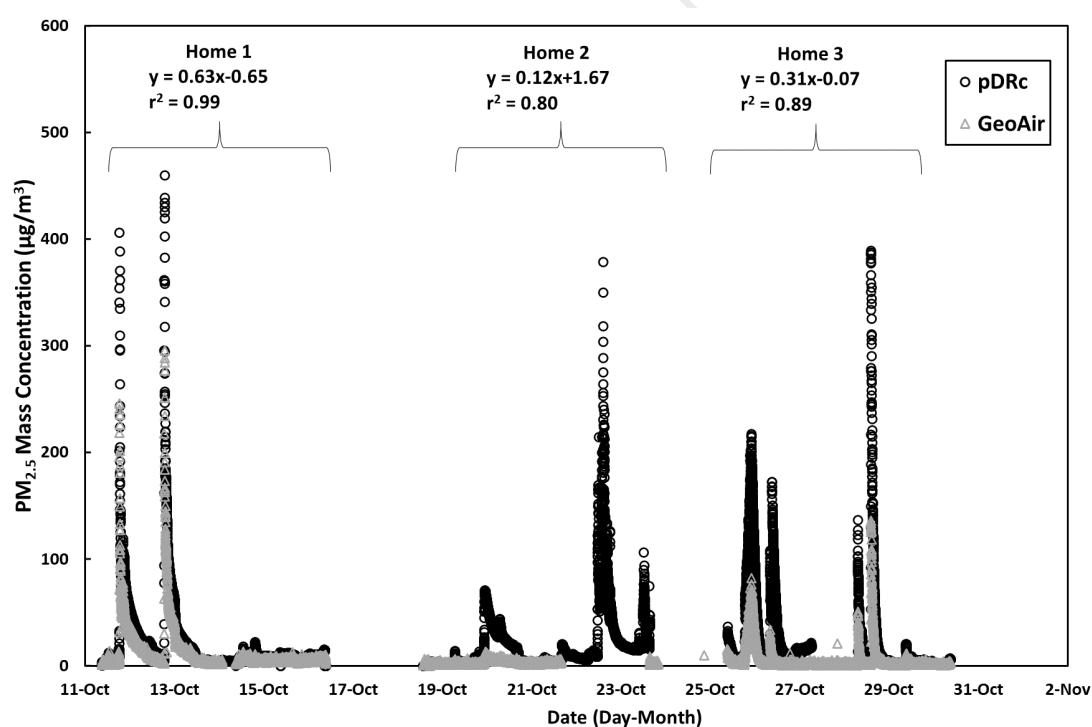


Figure 6. Time series plot of the filter-corrected pDR-1500 measurements and GeoAir2 measurements in three different indoor residential environments.

410

411

412 **4 CONCLUSIONS**

413

414 This study found that the GeoAir2 performed better than the higher-cost OPC-N3 for indoor
415 environments. In laboratory settings, the correlation with the MiniWRAS remained high across
416 both salt and ARD measurements. In addition, the GeoAir2 was less influenced by changes in
417 humidity when compared to the OPC-N3 during salt aerosol experiments. In indoor residential
418 environments, the GeoAir2 was highly correlated with the filter-corrected pDR-1500. These
419 findings suggest that the GeoAir2 is more suitable for indoor environments than the OPC-N3 due
420 to the more accurate results and lessened effect of changing environmental conditions (humidity).
421 Therefore, the GeoAir2 shows great potential for indoor air quality monitoring and exposure
422 assessments when calibrated on-site. Future work will focus on the outdoor environmental
423 evaluation of the GeoAir2.

424

425 **ACKNOWLEDGMENTS**

426 We would like to thank Dr. Jo Anne Balaney for her valuable feedback on this study.

427 **FUNDING**

428 This study was funded in part by the National Institute of Environmental Health Sciences
429 (NIEHS) under Award No. P30ES025128.

430

431 **Conflict of Interest**

432 The authors declare no competing financial interest

433

434 **ORCID**

435 Sinan Sousan: <https://orcid.org/0000-0001-5524-6911>

436

437

438

439

440

441

442

443 REFERENCES

444 Alphasense (2019). User Manual: OPC-N3 Optical Particle Counter, Issue 2.

445 Brook, R.D., Rajagopalan, S., Pope, C.A., Brook, J.R., Bhatnagar, A., Diez-Roux, A.V., Holguin,
446 F., Hong, Y., Luepker, R.V., Mittleman, M.A., Peters, A., Siscovick, D., Smith, S.C., Whitsel, L.,
447 Kaufman, J.D. (2010). Particulate matter air pollution and cardiovascular disease. *Circulation*
448 121, 2331-2378. <https://doi.org/doi:10.1161/CIR.0b013e3181dbee1>

449 Calvo, A.I., Alves, C., Castro, A., Pont, V., Vicente, A.M., Fraile, R. (2013). Research on aerosol
450 sources and chemical composition: Past, current and emerging issues. *Atmospheric Research*
451 120-121, 1-28. <https://doi.org/https://doi.org/10.1016/j.atmosres.2012.09.021>

452 Cincinelli, A., Martellini, T. (2017). Indoor air quality and health. *International journal of*
453 *environmental research and public health* 14, 1286. <https://doi.org/10.3390/ijerph14111286>

454 Collins, J.F., Salmon, A.G., Brown, J.P., Marty, M.A., Alexeeff, G.V. (2005). Development of a
455 chronic inhalation reference level for respirable crystalline silica. *Regul Toxicol Pharmacol* 43,
456 292-300. <https://doi.org/10.1016/j.yrtph.2005.08.003>

457 Crilley, L.R., Shaw, M., Pound, R., Kramer, L.J., Price, R., Young, S., Lewis, A.C., Pope, F.D.
458 (2018). Evaluation of a low-cost optical particle counter (Alphasense OPC-N2) for ambient air
459 monitoring. *Atmos. Meas. Tech.* 11, 709-720. <https://doi.org/10.5194/amt-11-709-2018>

460 Crilley, L.R., Singh, A., Kramer, L.J., Shaw, M.D., Alam, M.S., Apte, J.S., Bloss, W.J.,
461 Hildebrandt Ruiz, L., Fu, P., Fu, W., Gani, S., Gatari, M., Ilyinskaya, E., Lewis, A.C., Ng'ang'a,
462 D., Sun, Y., Whitty, R.C.W., Yue, S., Young, S., Pope, F.D. (2020). Effect of aerosol
463 composition on the performance of low-cost optical particle counter correction factors. *Atmos.*
464 *Meas. Tech.* 13, 1181-1193. <https://doi.org/10.5194/amt-13-1181-2020>

465 Demanega, I., Mujan, I., Singer, B.C., Anđelković, A.S., Babich, F., Licina, D. (2021).
466 Performance assessment of low-cost environmental monitors and single sensors under variable
467 indoor air quality and thermal conditions. *Build Environ* 187, 107415.
468 <https://doi.org/https://doi.org/10.1016/j.buildenv.2020.107415>

469 Diapouli, E., Chaloulakou, A., Mihalopoulos, N., Spyrellis, N. (2008). Indoor and outdoor PM
470 mass and number concentrations at schools in the Athens area. *Environ Monit Assess* 136, 13-20.
471 <https://doi.org/10.1007/s10661-007-9724-0>

472 Dubey, R., Patra, A.K., Joshi, J., Blankenberg, D., Kolluru, S.S.R., Madhu, B., Raval, S. (2022).
473 Evaluation of low-cost particulate matter sensors OPC N2 and PM Nova for aerosol monitoring.
474 *Atmos. Pollut. Res.* 13, 101335. <https://doi.org/https://doi.org/10.1016/j.apr.2022.101335>

475 EPA (1990). Criteria Air Pollutants: NAAQS Table. Accessed from the web in March 2021
476 [<https://www.epa.gov/criteria-air-pollutants/naaqs-table>].

477 EPA (2016). 40 CFR Parts 58- Ambient Air Quality Surveillance (Subchapter C).

478 Franklin, P.J. (2007). Indoor air quality and respiratory health of children. *Paediatric Respiratory*
479 *Reviews* 8, 281-286. <https://doi.org/https://doi.org/10.1016/j.prrv.2007.08.007>

480 GRIMM (2021). 1371 MiniWRAS, Portable mini wide range aerosol spectrometer [Accessed
481 from the web in December 2021: [https://www.grimm-aerosol.com/fileadmin/files/grimm-](https://www.grimm-aerosol.com/fileadmin/files/grimm-aerosol/3%20Products/Indoor%20Air%20Quality/The%20Wide%20Range%20Hybrid/1371/Product%20PDFs/Datasheet_1371miniwrass_ENG.pdf)
482 [aerosol/3%20Products/Indoor%20Air%20Quality/The%20Wide%20Range%20Hybrid/1371/Pro-](https://www.grimm-aerosol.com/fileadmin/files/grimm-aerosol/3%20Products/Indoor%20Air%20Quality/The%20Wide%20Range%20Hybrid/1371/Product%20PDFs/Datasheet_1371miniwrass_ENG.pdf)
483 [duct%20PDFs/Datasheet_1371miniwrass_ENG.pdf](https://www.grimm-aerosol.com/fileadmin/files/grimm-aerosol/3%20Products/Indoor%20Air%20Quality/The%20Wide%20Range%20Hybrid/1371/Product%20PDFs/Datasheet_1371miniwrass_ENG.pdf)].

484 Hansel, N.N., McCormack, M.C., Kim, V. (2016). The effects of air pollution and temperature on
485 COPD. *COPD* 13, 372-379. <https://doi.org/10.3109/15412555.2015.1089846>

486 Hong, G.-H., Le, T.-C., Tu, J.-W., Wang, C., Chang, S.-C., Yu, J.-Y., Lin, G.-Y., Aggarwal, S.G.,
487 Tsai, C.-J. (2021). Long-term evaluation and calibration of three types of low-cost PM_{2.5} sensors
488 at different air quality monitoring stations. *Journal of Aerosol Sci.* 157, 105829.
489 <https://doi.org/https://doi.org/10.1016/j.jaerosci.2021.105829>

490 Huang, K., Liang, F., Yang, X., Liu, F., Li, J., Xiao, Q., Chen, J., Liu, X., Cao, J., Shen, C., Yu,
491 L., Lu, F., Wu, X., Zhao, L., Wu, X., Li, Y., Hu, D., Huang, J., Liu, Y., Lu, X., Gu, D. (2019).
492 Long term exposure to ambient fine particulate matter and incidence of stroke: prospective cohort
493 study from the China-PAR project. *BMJ* 367, 16720. <https://doi.org/10.1136/bmj.16720>

494 Jiao, W., Hagler, G.S.W., Williams, R.W., Sharpe, R.N., Weinstock, L., Rice, J. (2015). Field
495 Assessment of the Village Green Project: An Autonomous Community Air Quality Monitoring
496 System. *Environ. Sci. Technol.* 49, 6085-6092. <https://doi.org/10.1021/acs.est.5b01245>

497 Kim, K.-N., Kim, S., Lim, Y.-H., Song, I.G., Hong, Y.-C. (2020). Effects of short-term fine
498 particulate matter exposure on acute respiratory infection in children. *Int. J. Hyg. Environ.* 229,
499 113571. <https://doi.org/https://doi.org/10.1016/j.ijheh.2020.113571>

500 Kulkarni, P., Baron, P.A., Willeke, K. (2011). Aerosol measurement: principles, techniques, and
501 applications. John Wiley & Sons

502 Levy Zamora, M., Xiong, F., Gentner, D., Kerkez, B., Kohrman-Glaser, J., Koehler, K. (2019).
503 Field and Laboratory Evaluations of the Low-Cost Plantower Particulate Matter Sensor. Environ.
504 Sci. Technol. 53, 838-849. <https://doi.org/10.1021/acs.est.8b05174>
505 Li, J., Li, W.X., Bai, C., Song, Y. (2017). Particulate matter-induced epigenetic changes and lung
506 cancer. Clin Respir J 11, 539-546. <https://doi.org/https://doi.org/10.1111/crj.12389>
507 Marć, M., Śmiełowska, M., Namieśnik, J., Zabiegała, B. (2018). Indoor air quality of everyday
508 use spaces dedicated to specific purposes—a review. Environ. Sci. Pollut. Res. 25, 2065-2082.
509 <https://doi.org/10.1007/s11356-017-0839-8>
510 Nguyen, N.H., Nguyen, H.X., Le, T.T.B., Vu, C.D. (2021). Evaluating low-cost commercially
511 available sensors for air quality monitoring and application of sensor calibration methods for
512 improving accuracy. Open J. Air Pollut Vol.10No.01, 17.
513 <https://doi.org/10.4236/ojap.2021.101001>
514 NIOSH (2012). Components for Evaluation of Direct-Reading Monitors for Gases and Vapors.
515 DHHS (NIOSH) Publication No. 2012–162. Cincinnati, OH: National Institute for Occupational
516 Safety and Health.
517 Owen, M.K., Ensor, D.S., Sparks, L.E. (1992). Airborne particle sizes and sources found in
518 indoor air. Atmos. Environ. Part A. General Topics 26, 2149-2162.
519 [https://doi.org/https://doi.org/10.1016/0960-1686\(92\)90403-8](https://doi.org/https://doi.org/10.1016/0960-1686(92)90403-8)
520 Park, Y.M., Sousan, S., Streuber, D., Zhao, K. (2021). GeoAir—a novel portable, GPS-enabled,
521 low-cost air-pollution sensor: design strategies to facilitate citizen science research and geospatial
522 assessments of personal exposure. SEN. 21, 3761. <https://doi.org/0.3390/s21113761>
523 Popoola, O.A.M., Carruthers, D., Lad, C., Bright, V.B., Mead, M.I., Stettler, M.E.J., Saffell, J.R.,
524 Jones, R.L. (2018). Use of networks of low cost air quality sensors to quantify air quality in urban
525 settings. Atmos. Environ. 194, 58-70.
526 <https://doi.org/https://doi.org/10.1016/j.atmosenv.2018.09.030>
527 Sensirion (2020). Datasheet SPS30: Particulate matter sensor for air quality monitoring and
528 control. Accessed from the web in March 2021
529 [https://www.sensirion.com/fileadmin/user_upload/customers/sensirion/Dokumente/9.6_Particiate_Matter/Datasheets/Sensirion_PM_Sensors_Datasheet_SPS30.pdf].
530
531 Slezakova, K., Castro, D., Pereira, M.C., Morais, S., Delerue-Matos, C., Alvim-Ferraz, M.C.
532 (2009). Influence of tobacco smoke on carcinogenic PAH composition in indoor PM10 and
533 PM2.5. Atmos. Environ. 43, 6376-6382.
534 <https://doi.org/https://doi.org/10.1016/j.atmosenv.2009.09.015>
535 Sousan, S., Gray, A., Zuidema, C., Stebounova, L., Thomas, G., Koehler, K., Peters, T. (2018).
536 Sensor selection to improve estimates of particulate matter concentration from a low-cost
537 network. SEN. 18. <https://doi.org/10.3390/s18093008>

538 Sousan, S., Koehler, K., Hallett, L., Peters, T.M. (2016a). Evaluation of the Alphasense optical
539 particle counter (OPC-N2) and the Grimm portable aerosol spectrometer (PAS-1.108). *Aerosol*
540 *Sci. Technol.* 50, 1352-1365. <https://doi.org/10.1080/02786826.2016.1232859>
541 Sousan, S., Koehler, K., Thomas, G., Park, J.H., Hillman, M., Halterman, A., Peters, T.M.
542 (2016b). Inter-comparison of low-cost sensors for measuring the mass concentration of
543 occupational aerosols. *Aerosol Sci. Technol.* 50. <https://doi.org/10.1080/02786826.2016.1162901>
544 Sousan, S., Regmi, S., Park, Y.M. (2021). Laboratory evaluation of low-cost optical particle
545 counters for environmental and occupational exposures. *SEN.* 21, 4146.
546 <https://doi.org/10.3390/s21124146>
547 Svenningsson, I.B., Hansson, H.C., Wiedensohler, A., Ogren, J.A., Noone, K.J., Hallberg, A.
548 (1992). Hygroscopic growth of aerosol particles in the Po Valley. *Tellus B: Chem. Phys.*
549 *Meteorol.* 44, 556-569. <https://doi.org/10.3402/tellusb.v44i5.15568>
550 Thermo. (2016). Model PDM3700 Personal Dust Monitor. Thermo Fisher Scientific. Available at
551 URL: <http://tools.thermofisher.com/content/sfs/manuals/EPM-manual-PDM3700.pdf>. Accessed
552 7, September 2018.
553 Tryner, J., Mehaffy, J., Miller-Lionberg, D., Volckens, J. (2020). Effects of aerosol type and
554 simulated aging on performance of low-cost PM sensors. *J Aerosol Sci* 150, 105654.
555 <https://doi.org/https://doi.org/10.1016/j.jaerosci.2020.105654>
556 Wang, P., Xu, F., Gui, H., Wang, H., Chen, D.-R. (2021). Effect of relative humidity on the
557 performance of five cost-effective PM sensors. *Aerosol Sci. Technol.* 55, 957-974.
558 <https://doi.org/10.1080/02786826.2021.1910136>
559 Wang, Y., Li, J., Jing, H., Zhang, Q., Jiang, J., Biswas, P. (2015). Laboratory evaluation and
560 calibration of three low-cost particle sensors for particulate matter measurement. *Aerosol Sci.*
561 *Technol.* 49, 1063-1077. <https://doi.org/10.1080/02786826.2015.1100710>
562 WHO (2010). Who Guidelines for Indoor Air Quality Selected Pollutants. [Accessed from the
563 web in July 2021: https://www.euro.who.int/__data/assets/pdf_file/0009/128169/e94535.pdf].
564 Zou, Y., Clark, J.D., May, A.A. (2021). A systematic investigation on the effects of temperature
565 and relative humidity on the performance of eight low-cost particle sensors and devices. *J*
566 *Aerosol Sci* 152, 105715. <https://doi.org/https://doi.org/10.1016/j.jaerosci.2020.105715>
567